

Supplementary Table 1. Variants numbers in different QC stages. S1: SNP-set after genotyping rate, missing rate in samples and monopolymorphism removing. S2: remove non-loss-of-functional related SNPs from S1 dataset.

Supplementary Table 2. All nonsynonymous SNV in FGF6 exon regions and missense mutation prediction with different algorithms.

Supplementary Table 3. Real-time PCR Primers for FGF6 network validation

Supplementary Figure 1. Two-Site Power Calculations. Power calculations for a two-site disease model comparing the Armitage trend test of disease association at each site to a log-likelihood ratio test explicitly evaluating recessive diplotype effects. Baseline haplotype frequencies, case and control diploid sample sizes, and relative risk of disease-predisposing diplotypes parameters are shown. The initial haplotype frequencies (A1B1, A1B2, A2B1, A2B2) are presented. Different combinations of haplotypes are generated by generating recombination between the two sites and the results are presented in a collapsed manner through a single linkage disequilibrium metric. Hardy-Weinberg equilibrium of haplotypes/diplotypes in the general population is assumed. R is the relative risk of disease for recessive diplotypes compared to the remaining diplotypes. ncs and nct are the number of cases and controls, respectively. The type I error rate, adjusted for an exome-wide scan, was set to 2.5E-06 for all calculations.

Supplementary Figure 2. Minor Allele Frequency Distribution to PMRP dataset. Displayed is the histogram of the minor allele frequency (MAF) at each variant within the 10,000 PMRP subjects following removal of variants from the QC procedures.

Supplementary Figure 3. Quantile-Quantile Plot. Q-Q plot for the exome-wide, gene-based recessive diplotype scanning in hemochromatosis is shown. Numerous genes had no recessive diplotypes with putative functional alleles and therefore yielded P-values of 1. The two data points exceeding the confidence interval represented *HFE* and *FGF6*.

Supplementary Figure 4. Comparative genomic analysis and protein-protein interaction (PPI). The comparative genomic analyses revealed that *FGF6* evolved synchronously with other iron metabolism genes. **(A)** Main iron metabolism genes were collected and alignment was conducted to make the comparative genomic analysis together with *FGF6*. The earliest gene appearance over time was inferred by comparing species and corresponding evolution and appearance time was labelled. **(B)** Protein-protein interaction network was estimated by String (version 10.0)^{SR1} using the highest confidence setting (confidence score>0.9).

Supplementary Figure 5. Total iron content in HFF-1 cells with increasing FGF-6 protein concentration.
* P<0.05; ** P<0.01. Results are the mean±SD of 3 observations in each experiment.

Supplementary Figure 6. FGF6 mutation Plasmid Structures in the study. M1 (GAG->TAG) E172X, M2 (GAC->GTC) D174V and M3 (CGG -> CAG) R188Q

Supplementary Figure 7. Perls' stain reveals that FGF6 loss-of-function nonsynonymous variants cause iron deposition. Perls' stain in HepG2 **(A)**, HCT-116 **(B)**, HCT-8 **(C)**, 786-O **(D)** and HFF-1 **(E)** in the presence of FAC differs among transfection by *FGF6* mRNA with wildtype and the identified variants R188Q, D174V and E172X.

Supplementary figure 8. FGF6 loss-of-function nonsynonymous variants cause hepcidin downregulation and iron deposition in HFF-1. **(A)** Iron metabolism gene expression changes after the transfection by *FGF6* mRNA into HFF-1 with wildtype and the identified variants R188Q, D174V and E172X. **(B)** Total iron contents changes after the transfection by *FGF6* mRNA into HFF-1 with wildtype and the identified variants R188Q, D174V and E172X. **(C)** Ferritin protein level changes after the transfection by *FGF6* mRNA into HFF-1 with wildtype and the identified variants R188Q, D174V and E172X. **(D)** The densitometry data of Western blot for Ferritin protein were shown in the column chart. *P<0.05; **P<0.01. Results are the mean±SD of three observations in one experiment.

Supplementary figure 9. Perls' stain in SSc and liver cancer. (A) Perls' stain was applied to evaluate the iron deposition in SSc skin tissues. Perls' stain was visualized by Nikon microscopy. The ratio of iron-positive stain areas to the total area was used to evaluate the iron deposition levels by Image J software. Arrows indicated positive stain area. (B) Perls' stain in liver cancer tissues. Perls' stain was visualized by Nikon microscopy. The ratio of iron-positive stain areas to the total area was used to evaluate the iron deposition levels by Image J software.

Supplementary figure 10. FGF-6 protein levels were different among normal, cancer and metastatic cells. (A) IHC of FGF-6 in normal hepatocytes and metastatic cells. The blue circle indicated normal liver tissue and the arrows indicated metastatic cells. (B) IHC of FGF-6 in non-metastatic liver cancer cells.

Supplementary figure 11. Relative transcription of iron metabolism genes with wildtype *FGF6* and three mutations. mRNA levels of *FGF6* and four iron metabolism genes are measured relative to *GAPDH* following transfection of vector, wildtype *FGF6* (WT), E172X *FGF6* (M1), D174V *FGF6* (M2), and R188Q *FGF6* (M3). Measurements were taken in three cell lines: 786-O, A498, and HCT-8.

Supplemental Reference

SR1. Szklarczyk, D. *et al.* STRING v10: protein-protein interaction networks, integrated over the tree of life. *Nucleic Acids Res* **43**, D447-52 (2015).

Supplementary Table 1. Variants numbers in different QC stages

MAF Internal	No#	Freq%	S1	S2
0	126400	0.221892582		
0-0.001	99512	0.174691255		84360
0.001–0.005	24629	0.043235699		18428
0.005–0.01	7717	0.013547034		5023
0.01–0.05	22547	0.039580792		8102
>0.05	259296	0.455188758		13643
	413701		129556	P=0.22

S1: SNP-set after genotyping rate, missing rate in samples and monopolymorphism removing.

S2: remove non-loss-of-functional related SNPs from S1 dataset.

S. Table 2. All nonsynonymous SNV in FGF6 exon regions and missense mutation prediction with different algorithms.

Chr	Start	End	Alt	Func.refGene	Gene.refGene	GeneDetail.refGene	AAChange.refGene	phastConsElements46way	Polyphen2_HDIV	Polyphen2_HVAR	LRT	MutationTaster	MutationAssessor	FATHMM	PROVEAN	VEST3	MetaLR	M-CAP	CADD
12	4543445	C	T	exonic	FGF6	nonsynonymous SNV	FGF6.NM_020996.exon3:c.G563A.p.R188Q	D	D	D	D	L	T	N	T	T	D	D	
12	4543487	T	A	exonic	FGF6	nonsynonymous SNV	FGF6.NM_020996.exon3:c.A521T.p.D174V	T	B	B	N P	N	T	N	T	T	.	N	
12	4543494	C	A	exonic	FGF6	stopgain	FGF6.NM_020996.exon3:c.G514T.p.E172X	.	.	D D	D	
12	4543523	G	A	exonic	FGF6	nonsynonymous SNV	FGF6.NM_020996.exon3:c.C485T.p.T162I	T	B	B	N D	N	D	N	T	T	T	D	
12	4553300	G	A	exonic	FGF6	nonsynonymous SNV	FGF6.NM_020996.exon2:c.C449T.p.T150M	D	D	D D	M	D	D	D	D	D	D	D	
12	4553304	C	T	exonic	FGF6	nonsynonymous SNV	FGF6.NM_020996.exon2:c.G445A.p.A149T	T	B	B	N N	L	D	N	T	T	D	D	
12	4553361	G	C	exonic	FGF6	nonsynonymous SNV	FGF6.NM_020996.exon2:c.C388G.p.L130V	D	D	P	D D	M	D	N	D	D	D	D	
12	4553391	T	C	exonic	FGF6	nonsynonymous SNV	FGF6.NM_020996.exon2:c.A358G.p.I120V	D	P	P	D D	L	D	N	D	D	D	D	
12	4554550	C	T	exonic	FGF6	nonsynonymous SNV	FGF6.NM_020996.exon1:c.G187A.p.A63T	T	B	B	N N	L	T	N	T	T	.	N	
12	4554630	A	G	exonic	FGF6	nonsynonymous SNV	FGF6.NM_020996.exon1:c.T107C.p.V36A	T	B	B	N P	L	T	N	T	T	.	D	
12	4554651	C	A	exonic	FGF6	nonsynonymous SNV	FGF6.NM_020996.exon1:c.G86T.p.G29V	D	P	B	D D	L	T	N	T	T	T	D	

Supplementary Table 3. Real-time PCR Primers for FGF6 network validation

No.	Gene symbol	Accession number	Forward primer	Reverse primer	Forward TM	Reverse TM	Amplicon size
1	HAMP	NM_021175.3	CTGACCAGTGGCTCTGTTTCC	AAGTGGGTGTCTCGCCTCCTTC	61.39	64.21	128
5	HDAC2	NM_001527.3	AGCCACTGCCGAAGAAATGA	AACTTCACAGCTCCAGCACT	59.68	59.86	198
24	GAPDH	NM_001289745.2	GAGTCAACGGATTGGTCGT	CATGGGTGGAATCATATTGGA	58.21	55.39	141
25	FGF6	NM_020996.2	GTGCCCTCTTCGTTGCC	TACCCGTCCGTATTGCT	58.3	55.58	164
26	HEPH	NM_001130860.3	CAGGTGGTCTTCTACAACCGTG	TGGCAACCAAGCCAGGGTAAGA	60.87	64.17	124
27	TFRC	NM_001313966.1	ATCGGTTGGTGCCACTGAATGG	ACAACAGTGGGCTGGCAGAAC	63.42	63.8	131

Figure S1

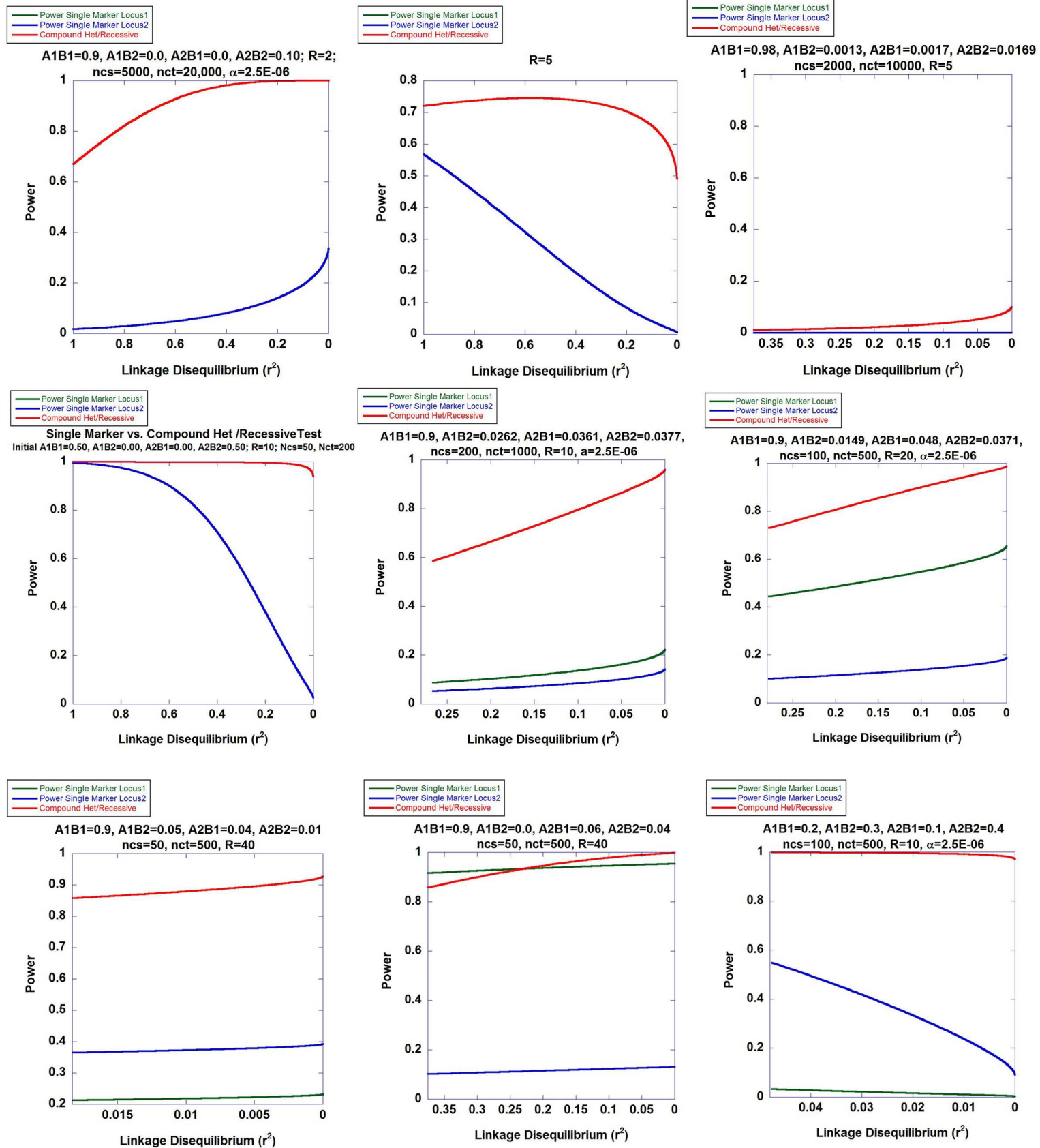


Figure S2

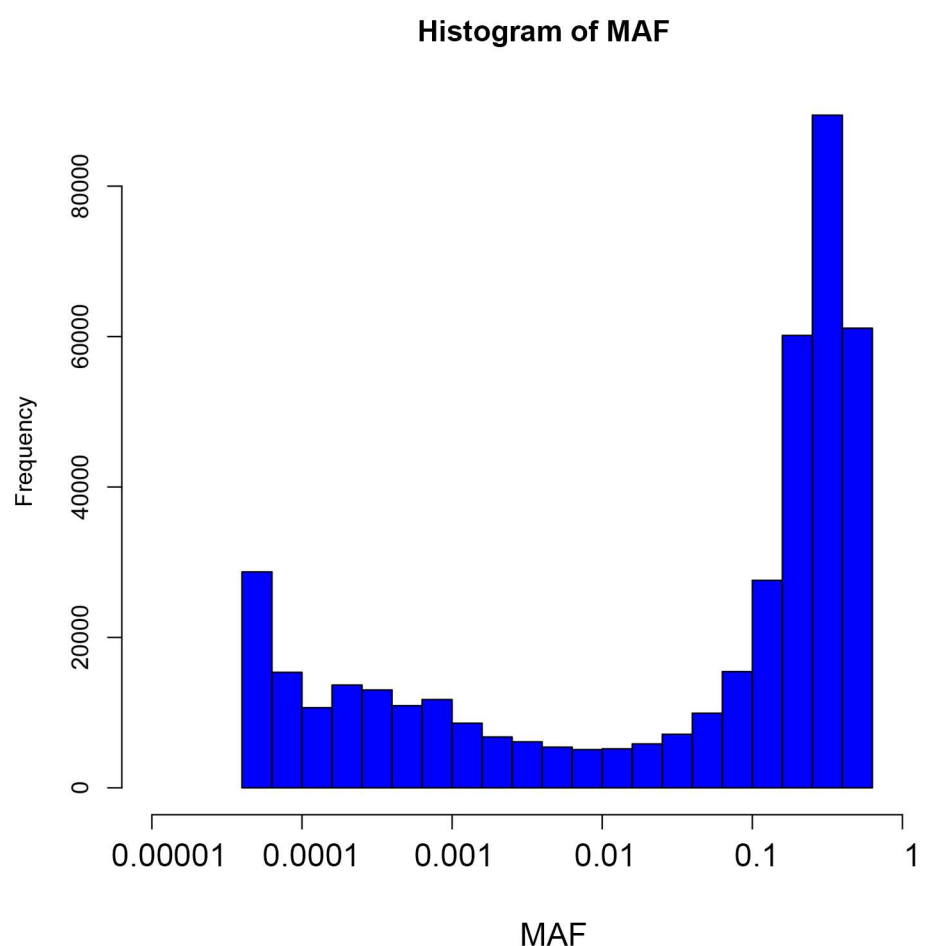


Figure S3

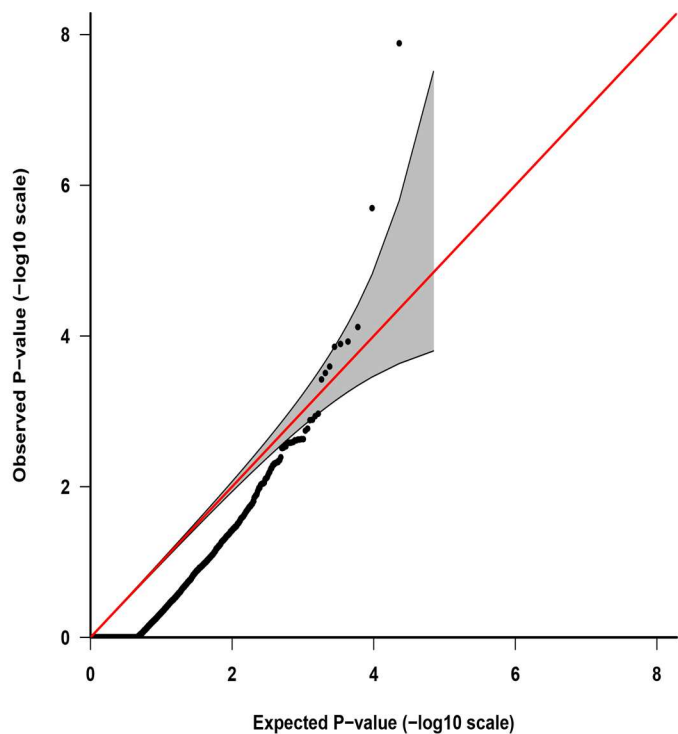


Figure S4

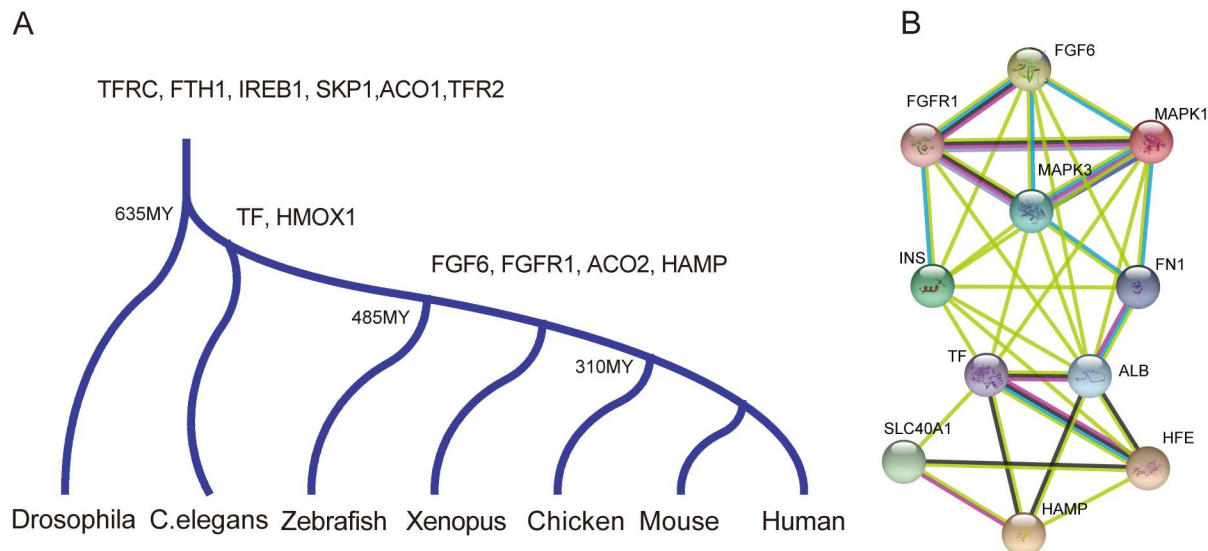


Figure S5

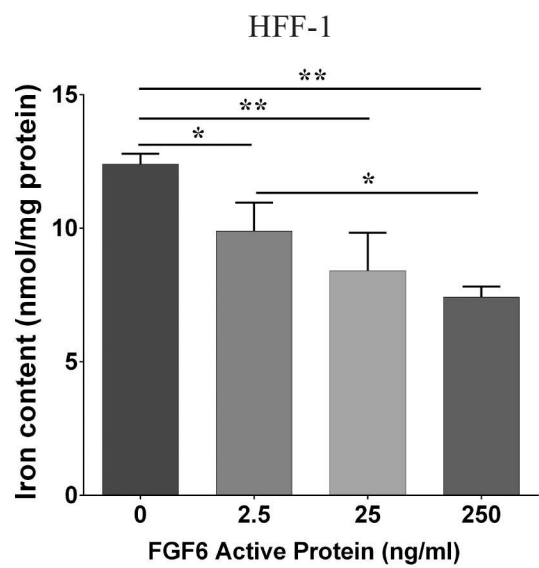


Figure S6

FGF6 Mutation Plasmid Structure

M1 Plasmid [GAG -> TAG] **E172X**

```
ATGGCCCTGGACAGAAACTGTTCATCACTATGTCCGGGGAGCA  
GGACGTCTGCAGGGCACGCTGTGGCTCTCGTCTTCCTAGGCATCC  
TAGTGGCATGGTGGTGCCTCGCCTGCAGGCACCCGTGCCAAC  
ACACGCTGGAACGGCTGGGACCCCTGCTGTCCAGGT  
CTCGCGCCGGCTAGCTGGAGAGATTGCCGGGGTAACCTGCTGTCCAGGT  
GTGGCTATTGGTGGGATCAAGCGCAGCGGAGGCTACTGCA  
ACGTGGGCATCGGCTTCACCTCAGGTGCTCCCCGACGGCCGA  
TCAGCGGGACCCACGAGGAGAACCCCTACAGCCTGCTGGAAATT  
CCACTGTGGAGCGAGGCGTGGTGAAGTCTTGGAGTGAGAAGTG  
CCCTCTCGTTGCCATGAACAGTAAAGGAAGATTGTACCGAACGCC  
CAGCTTCCAAGAAGAATGCAAGTTCAAGAGAAACCCCTGCCAAC  
CAATTACAATGCCTACTAGTCAGACTTGTACCAAGGGACCTACATT  
GCCCTGAGCAAATACGGACGGTAAAGCGGGCAGCAAGGTGTC  
CCCGATCATGACTGTCACTCATTCCCTCCCAGGATCTAA
```

Point Mutation Construct Primers

F1 : ATACTCGGATCCGCCACCATG
R1 : CTTGGTACAAGTCTGACTAGTAGGCATTG
F2 : CAATGCCTACTAGTCAGACTTGTACCAAG
R2 : GCTGCAGAATTCTTACGTAATCTGGAA

FGF6 Mutation Plasmid Structure

M2 Plasmid [GAC -> GTC] **D174V**

```
ATGGCCCTGGACAGAAACTGTTCATCACTATGTCCGGGGAGCA  
GGACGTCTGCAGGGCACGCTGTGGCTCTCGTCTTCCTAGGCATCC  
TAGTGGCATGGTGGTGCCTCGCCTGCAGGCACCCGTGCCAAC  
ACACGCTGGAACGGCTGGGACCCCTGCTGTCCAGGT  
CTCGCGCCGGCTAGCTGGAGAGATTGCCGGGGTAACCTGCTGTCCAGGT  
GTGGCTATTGGTGGGATCAAGCGCAGCGGAGGCTACTGCA  
ACGTGGGCATCGGCTTCACCTCAGGTGCTCCCCGACGGCCGA  
TCAGCGGGACCCACGAGGAGAACCCCTACAGCCTGCTGGAAATT  
CCACTGTGGAGCGAGGCGTGGTGAAGTCTTGGAGTGAGAAGTG  
CCCTCTCGTTGCCATGAACAGTAAAGGAAGATTGTACCGAACGCC  
CAGCTTCCAAGAAGAATGCAAGTTCAAGAGAAACCCCTGCCAAC  
CAATTACAATGCCTACGAGTCAGTCTTGTACCAAGGGACCTACATT  
GCCCTGAGCAAATACGGACGGTAAAGCGGGCAGCAAGGTGTC  
CCCGATCATGACTGTCACTCATTCCCTCCCAGGATCTAA
```

Point Mutation Construct Primers

F1 : ATACTCGGATCCGCCACCATG
R1 : GGTACAAGACTGACTCGTAGGCATTG
F2 : CTACGAGTCAGTCTTGTACCAAGGG
R2 : GCTGCAGAATTCTTACGTAATCTGGAA

FGF6 Mutation Plasmid Structure

M3 Plasmid [CGG ->CAG] **R188Q**

```
ATGGCCCTGGACAGAAACTGTTCATCACTATGTCCGGGGAGCA  
GGACGTCTGCAGGGCACGCTGTGGCTCTCGTCTTCCTAGGCATCC  
TAGTGGCATGGTGGTGCCTCGCCTGCAGGCACCCGTGCCAAC  
ACACGCTGGAACGGCTGGGACCCCTGCTGTCCAGGT  
CTCGCGCCGGCTAGCTGGAGAGATTGCCGGGGTAACCTGCTGTCCAGGT  
GTGGCTATTGGTGGGATCAAGCGCAGCGGAGGCTACTGCA  
ACGTGGGCATCGGCTTCACCTCAGGTGCTCCCCGACGGCCGA  
TCAGCGGGACCCACGAGGAGAACCCCTACAGCCTGCTGGAAATT  
CCACTGTGGAGCGAGGCGTGGTGAAGTCTTGGAGTGAGAAGTG  
CCCTCTCGTTGCCATGAACAGTAAAGGAAGATTGTACCGAACGCC  
CAGCTTCCAAGAAGAATGCAAGTTCAAGAGAAACCCCTGCCAAC  
CAATTACAATGCCTACGAGTCAGACTTGTACCAAGGGACCTACATT  
GCCCTGAGCAAATACGGACAGGTAAGCGGGCAGCAAGGTGTC  
CCCGATCATGACTGTCACTCATTCCCTCCCAGGATCTAA
```

Point Mutation Construct Primers

F1 : ATACTCGGATCCGCCACCATG
R1 : CGCTTACCTGTCCGTATTGCTC
F2 : GAGCAAATACGGACAGGTAAAGCG
R2 : GCTGCAGAATTCTTACGTAATCTGGAA

Figure S7

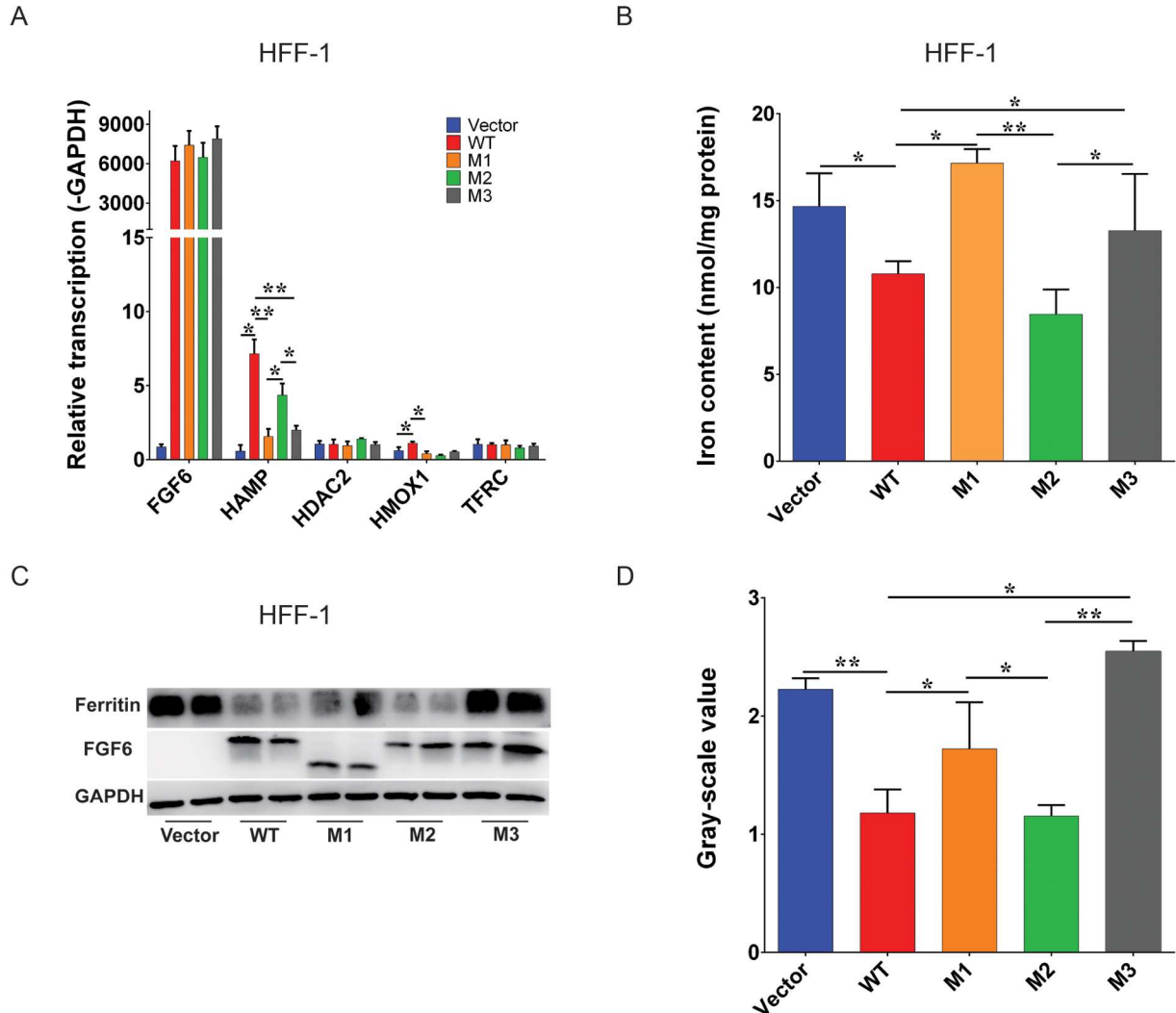


Figure S8

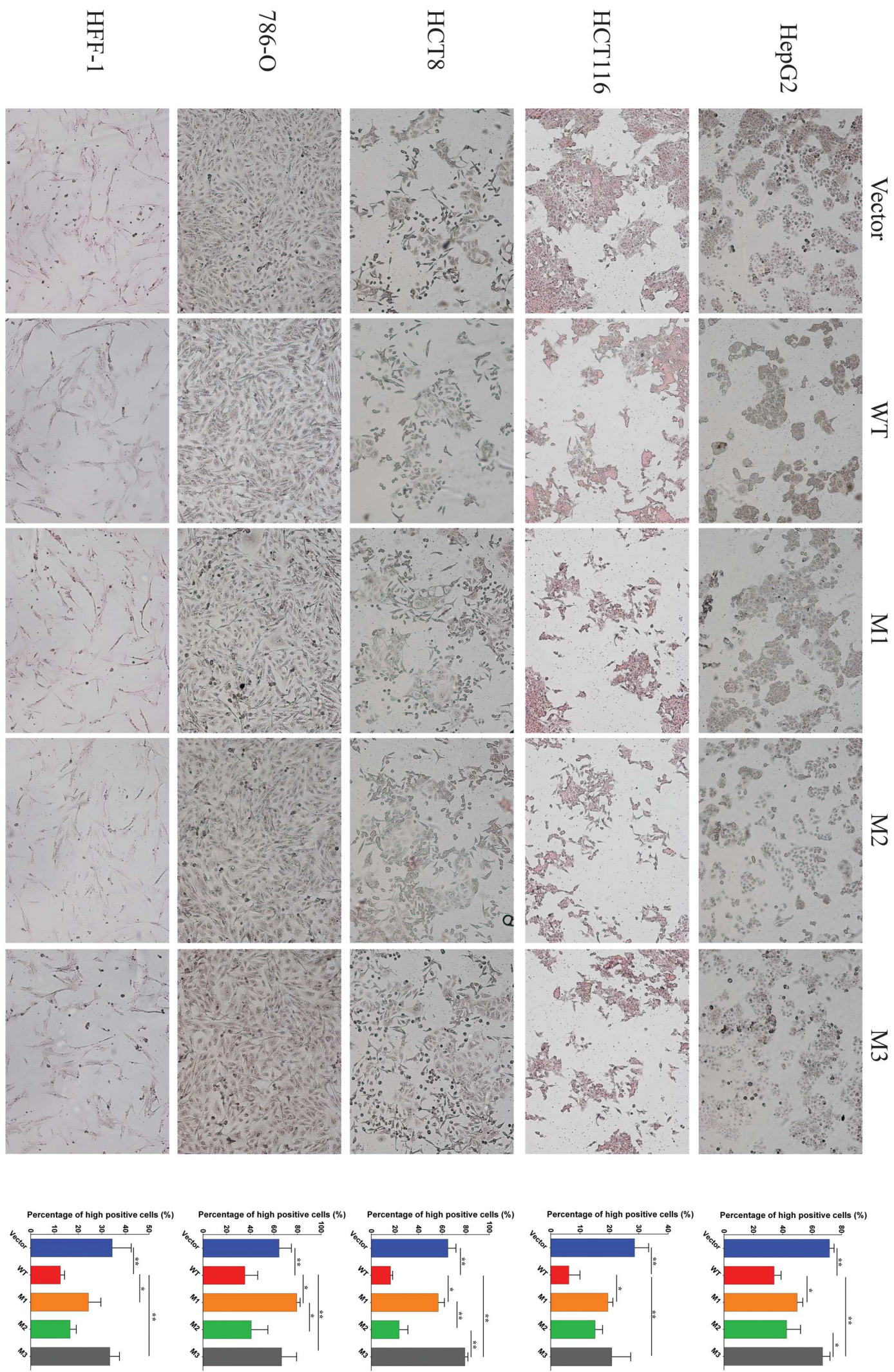
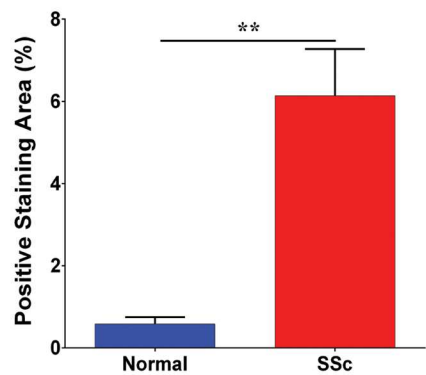
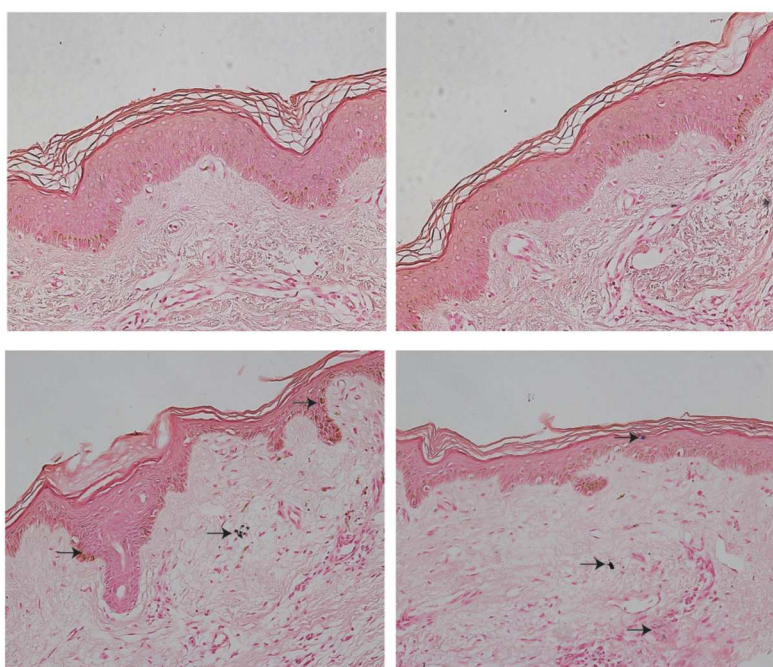


Figure S9

A



B

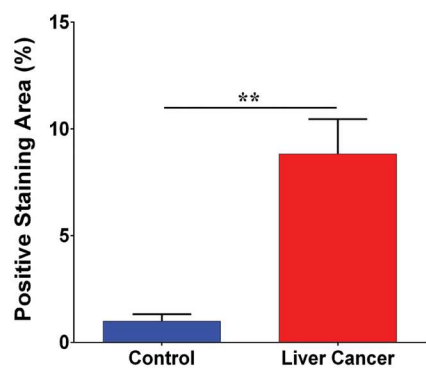
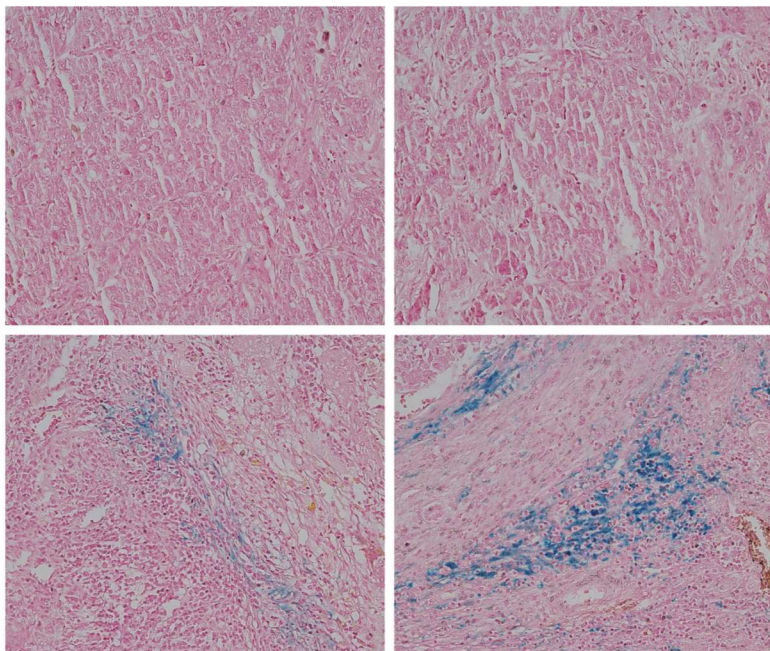


Figure S10

A (normal hepatocytes and metastatic cells) B (non-metastatic liver cancer cells)

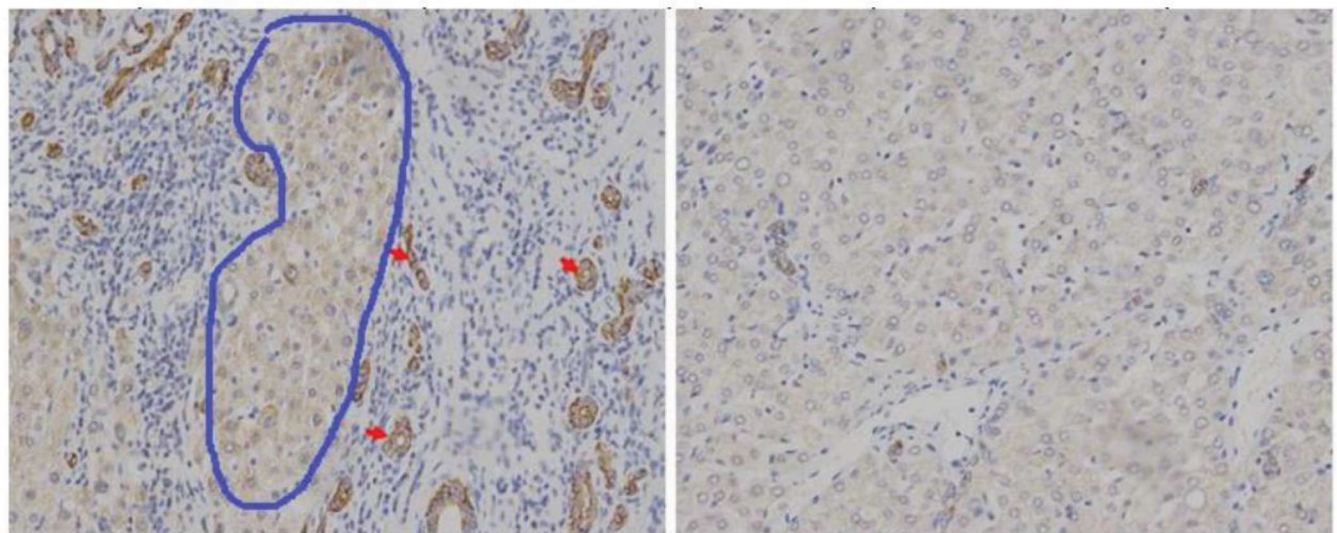


Figure S11

